J Mater Sci (2009) 44:5459–5468
DOI 10.1007/s10853-009-3745-8

Kinetic study of controlled release of VPA and DPH antiepileptic drugs using biocompatible nanostructured sol–gel TiO_2

T. López · R. Alexander-Katz · P. Castillo · M. González · J. Manjarrez · R. D. Gonzalez · L. Ilharco · A. Fidalgo · J. Rieumont

Received: 17 December 2008 / Accepted: 15 July 2009 / Published online: 6 August 2009

Abstract Sol–gel TiO_2 porous matrix was used to host valproic acid (VPA) and phenytoin (DPH), which are commonly used as antiepileptic drugs. The addition of these drugs was carried out during the synthesis in the hydrolysis stage. In vitro short term kinetic studies on drug liberation showed that almost all samples followed a first order kinetics with the exception of one sample which had a linear behavior. High resolution electron microscopy revealed the existence of nanocrystalinity in all samples, however, electron diffraction patterns showed that some were predominantly amorphous while in others suggested a greater density of nanocrystals. NMR studies demonstrated that VPA was less mobile in a more crystalline TiO_2 matrix than when the TiO_2 is mainly amorphous. Some features of the kinetics of drug liberation are explained in terms of the competition between nanocrystallinity and drug content. The reservoirs were implanted by means of stereotactic surgery in Wistar rats in which epilepsy was previously induced following the Kindling model of epilepsy. The efficiency of the reservoirs was follow by electroencephalography (EEGs). In vivo studies revealed that a more crystalline sample was more effective in preventing further epileptic events than samples with a higher content of VPA but predominantly amorphous.

Introduction

The blood–brain barrier (BBB) represents an insurmountable obstacle for a large number of drugs. However, one of the possibilities that may be used to overcome this barrier is local drug delivery using nanoparticles in the damaged areas of the brain [1]. Biocompatible nanostructured-release inorganic materials offer an alternative to local

T. López
Departamento de Atención a la Salud, Universidad, Autónoma Metropolitana-Xochimilco, Calzada del Hueso 1100, Col. Villa Quietud, Delegación Coyoacán, C. P. 04960 México, D.F., México

T. López (✉) · J. Manjarrez
Instituto Nacional de Neurología y Neurocirugía MVS, Insurgentes Sur No. 3877 Col. La Fama, C. P. 14269 Tlalpan, México, D.F., México
e-mail: tessy3@prodigy.net.mx

T. López · R. D. Gonzalez
Department of Chemical and Bimolecular Engineering, Tulane University, New Orleans, LA 70118, USA

R. Alexander-Katz
Departamento de Física, Universidad Autónoma Metropolitana-Iztapalapa, Av. San Rafael Atlixco 186, Col. Vicentina, C.P. 09340 Iztapalapa, México, D.F., México

P. Castillo
Laboratorio Central, Universidad Autónoma Metropolitana-Iztapalapa, Av. San Rafael Atlixco 186, Col. Vicentina, C.P. 09340 Iztapalapa, México, D.F., México

M. González
Engineering and Chemical Research Center, C.P. 10600 Havana City, Cuba

L. Ilharco · A. Fidalgo
Centro de Quimica-Fisica Molecular, Complexo I, Instituto Superior Tecnico, Av. Rovisco Pais, Pt-1049-001 Lisbon, Portugal

J. Rieumont
Dept. of Physical Chemistry, University of La Havana, C.P. 10600 Havana City, Cuba

delivery in the temporal lobe near the epileptic focus. In recent years, several approaches have been used to obtain controlled drug delivery systems due to their potential advantages over conventional drug therapy [2]. These delivery systems can be localized in a specific area in the body achieving prolonged pharmacological effects while lowering the systemic concentrations of drugs. Various types of carriers for drug delivery systems have been reported. These include polymers, liposomes, dendrimers [3], and inorganic materials [1, 4, 5]. In the case of epilepsy, inorganic implants have advantages over the other materials since they can be extracted easily after most of the drug has been delivered and substituted for a new one. Inorganic reservoirs have good properties, suitable for drug delivery such as good biocompatibility, easy functionalization, and potential capability for targeted delivery and controlled release of encapsulated drugs.

In a previous work [6], a long term in vitro release study was performed at room temperature showing some striking features, that is, for valproic acid (VPA) at higher loadings of the drug the initial release was considerably lower than at lower loadings. The same occurs with the highest concentration used of phenytoin (DPH), its initial delivery is smaller than the samples with a lower concentration of the drug. It was also observed that for VPA the rate of delivery of the two samples with the highest loadings differ notably in spite that both samples were quite similar in preparation and in their textural parameters.

In this study, we analyze in detail the short term delivery kinetics of the same systems of VPA and DPH encapsulated and stabilized in titania matrix during the sol–gel synthesis as in Peterson et al. [6]. "In vitro" short term release kinetics was studied in accordance with USP XXVII procedures [7]. High resolution transmission electron microscopy (HRTEM) characterization on the crystallization of these systems threw light on some possible mechanism by which the release of these drugs from the titania reservoirs have the features described above. In vivo studies were performed on the animals using the Kindling model of epilepsy as well as behavioral and electroencephalographic studies and there efficiency in preventing further epileptic events was correlated with the HRTEM results.

Materials and methods

Sample preparation

Sol–gel TiO_2 reservoirs containing VPA or DPH were synthesized following the same procedure as in Ref. [6]. Four 20 g xerogel samples were synthesized by sol–gel methods with 200, 400, 800 and 1000 mg of VPA which from now on will be named VPA200, VPA400, VPA800, and VPA1000, respectively. VPA was dissolved in a mixture of 190 mL of *tert*-butanol and 36 mL of water under constant stirring at room temperature. The final solution had a pH of 2. After that, 87 mL of titanium *n*-butoxide was added dropwise over a 4 h period. The resulting sols were maintained under constant stirring for 24 h. The total molar ratio of water/alkoxide/alcohol was 8/1/8. In the case of the TiO_2–DPH samples, three 20 g xerogels were prepared with 50, 100, 250 mg of DPH which from now on will be named DPH50, DPH100, and DPH250, respectively. Sodium phenytoin was diluted in a mixture of water and ethanol then added dropwise in a mixture of 85.08 g of titanium *n*-butoxide and 57.5 mL of ethanol. The total molar ratio of water/alkoxide/alcohol was the same as before. The mixture was maintained at a pH of 12 during gelation. In all cases, the excess water and alcohol were removed from the gel by means of a rotary evaporator and finally the gels were dried at 30 °C for a week.

Transmission electron microscopy

High resolution TEM microstructural characterization was made in a field emission electron microscope FEI F-30 of 300 Kv by Phillips. On the other hand, all the electron diffraction patterns here presented were performed in a Zeiss EM910 of 120 Kv at a lower amplification in order to choose a more representative area.

Solid state NMR

NMR studies on samples with VPA were performed with a Bruker Instrument model Advance II-300 using a 4 mm CP-MAS probe (31P-15N) at 5 KHz. Only the samples VPA800 and VPA1000 with the highest drug concentration were susceptible of NMR studies.

In vitro release studies

In vitro release studies were performed in accordance with the standard USP 30 [7], in a type II apparatus at 100 rpm and at a temperature of 37 ± 0.2 °C. The encapsulated antiepileptic drug was suspended in 100 mL degasified mixture of 0.1 N of HCl and 0.2 M of Na_3PO_4(3:1). The release of the drug was monitored each 2 h for 22 h by means of HPLC with a KNAUER apparatus equipped with a Smartline PDA detector 2800 UV/VIS/NIR.

"In vivo" studies

For this purpose male Wistar rats (180–250 g) were used in this study. All rats were induced epileptic convulsions

following the Kindling model, that is, the rats were intraperitoneally injected with a subconvulsive dose of Pentilentetrazole (PTZ) (35 mg/kg) in saline solution. After each injection, observations were made for 20 min and the resulting seizures classified: No response = 0; facial and ear trembling = 1; anterior limb and facial trembling = 2; myoclonic trembling and rising = 3; clonic convulsions with animal tipping on side = 4; and severe repetitive tonic–clonic convulsions = 5. The animals were considered as kindled after exhibiting at least three consecutive level 4 or 5 seizures [8]. After this stage, the rats were allowed to recover for a period of 7 days. The reservoir was then implanted and evaluations were made by means of electroencephalography (EEG) to study the effects of the TiO_2-sol–gel–VPA reservoir in the seizure-induced changes.

The implantation of the antiepileptic reservoir in the temporal lobe of a rat was performed using stereotaxic surgery. The external reference was the location of the Bregma. The reservoir is cylindrical in shape with 1 mm in diameter and 1.2 mm in height weighing 1.3 mg. and was inserted at the coordinates AP = −2.3; $L = 4.8$; $V = 8.5$ [9].

For VPA, concentration of 200, 400, and 1000 mg were used while for DPH we only report the results for DPH100. For each concentration 24 rats were implanted including a reference group of six with an empty TiO_2 reservoir (no drug). The individual rats were maintained in a room with a light/dark period of 12 h under controlled temperature and humidity conditions [10]. The rats had ad libitum access to water and food. Experiments were performed in accordance with the ethical rules for treatment of animals of the Mexican Ministry of Health and approved by the local animal committee for animal care.

Histopathological studies

A group of rats was killed using an overdose of sodium phenobarbital administered by an intraperitoneal injection after 6 months following the implant. After that they were perfused using a saline solution of 3.7% formaldehyde. The brains were extracted and conserved in 3.7% formaldehyde solution. The brain specimens were microtomed and conserved in a 4% formaldehyde solution for a period of 15 days. Sections (10 μm) were embedded in paraffin and viewed using an optical microscope. The sections were dyed using the Bielchowsky technique, which enables viewing the neuronal microfibrils and cell soma integrity. Implant position did not vary after 6 months in the basolateral amygdala, meaning that the reservoir was highly compatible with the nervous tissue. To confirm the lack of glial response to the implant, sections were taken of the implant zone for histological analysis and neuronal damage evaluation.

Results and discussion

Drug delivery "in vitro" studies

Figures 1 and 2 show the kinetics of drug delivery for DPH and VPA, respectively. With the exception of sample with

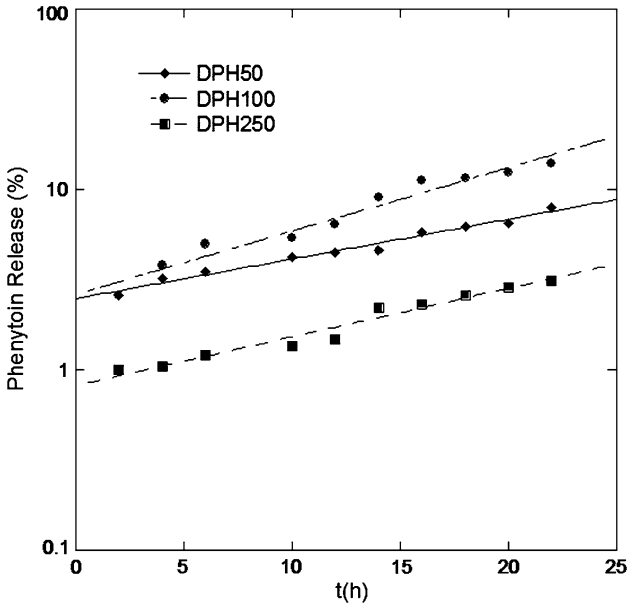

Fig. 1 Release profiles for the TiO_2–DPH

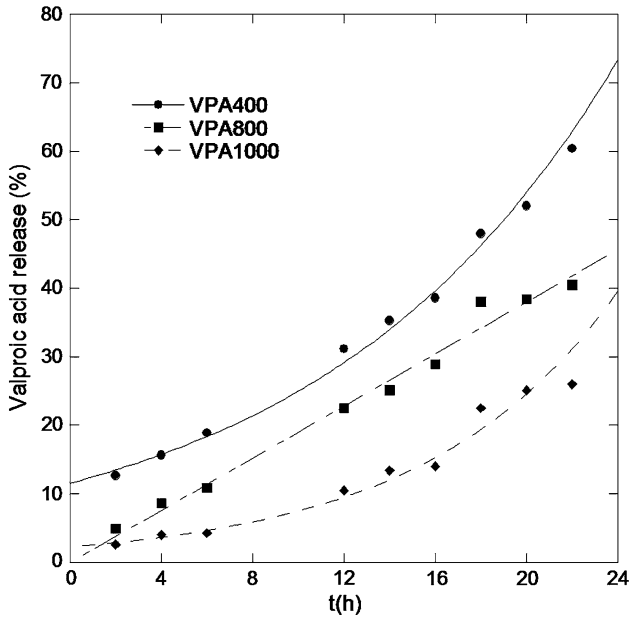

Fig. 2 Release profiles for the TiO_2–VPA

800 mg of VPA (VPA800), all the rest follow a first order kinetics, that is, they are well represented by an exponential growth. In contrast, the kinetics of sample VPA800 is of zero order so that the rate of delivery is constant and independent of the concentration, which implies that the dominating mechanism is not related with concentration gradients between the reservoirs and the fluid surrounding it.

In the case of DPH, the samples DPH50 and DPH100 have an early overshoot of phenytoin weakly bound and reach a specific level in the first 2 h. It is observed that for sample DPH250 the first 2 h overshoot is smaller than the other samples following the same pattern as in Peterson et al. [6]. After 2 h, samples DPH50, DPH100, and DPH250 follow an exponential liberation growth with rate constants 0.051, 0.081, and 0.062 h^{-1}, respectively. As one can see from Table 1 (taken from reference [6]) the presence of phenytoin in the sol–gel reaction of TiO_2 hardly reflects on a change in pore size and surface area. Therefore, one cannot attribute the delivery pattern to pore size.

On the other hand, samples VPA400 and VPA1000 present also an early delivery within the first 2 h of weakly adsorbed VPA, this being larger for sample VPA400. After that, both samples show an exponential growth type of drug delivery with rate constants for VPA400 and VPA1000 of 0.077 and 0.119 h^{-1}, respectively. In contrast, the kinetics of drug release of sample VPA800 follow a linear law from the start with a constant rate of 1.9%/h. As in the long term study, the release of VPA800 always falls below that of VPA400. In this interval of time sample, VPA1000 deliver less than the rest, however, at the end of the period analyzed sample VPA1000 will release about the same amount than VPA800 surpassing it at higher times which is consistent with what is observed at greater times [6].

Table 1 A comparison of the best fit values for surface areas *S* and pore diameter for DPH filled samples using Joyner *n* equation

Phenytoin (mg)	*S* (m^2/g) Joyner et al.	Pore diameter (nm) Joyner et al.
0	504	4.0
50	497	4.2
250	538	4.1

Adapted from [6] with permission

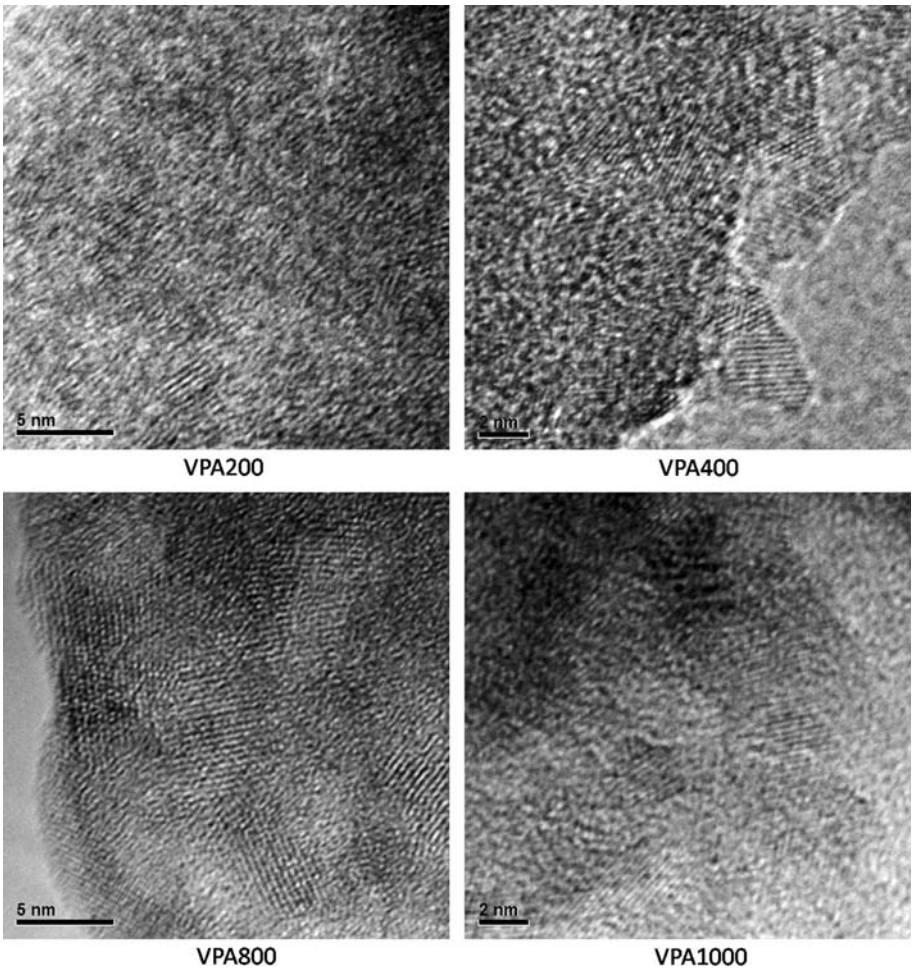

Fig. 3 HRTEM of samples of TiO_2 with different contents of VPA

High resolution electron microscopy and NMR

Figures 3 and 4 show HRTEM micrographs of samples with VPA and DPH, respectively. It has been chosen regions where the crystalline structures are evident to show that in all cases small crystallites are formed. However, there are large zones where apparently nonorganized structure prevail. On the other hand, Figs. 5 and 6 illustrate some typical diffraction patterns of the systems with VPA and DPH, respectively, with the exception of sample DPH50 where the diffraction patterns differ notoriously from zone to zone as shown in Fig. 6. All diffraction patterns were taken at a lower amplification in order to be representative of a larger zone of the material. However, in spite of the latter, each zone differed from one and other, and it is difficult to index in a unique way the different diffraction patterns found for each sample. In general, one could say that most of them share some of the reflections proper of a sol–gel titania in an anatase crystalline form. Nonetheless, their difference from anatase confirm the effect of the drug in the crystallization process producing crystallites which are smaller than 5 nm and therefore difficult to observe by X-ray as shown in Fig. 7. However, there are some differences between samples; while in all of them there are small crystals present some of them have well defined diffraction patterns and others a diffuse and broad diffraction rings prevail. This is the case of TiO_2–VPA where samples VPA200 and VPA800 have well defined diffraction patterns all over the sample while samples VPA400 and VPA1000 present diffuse diffraction patterns with broad diffraction rings as shown in Fig. 5. It is not clear why for some specific concentrations of VPA the crystallites are more homogeneous or more abundant than the amorphous zones or both. Given the way these reservoirs were synthesized, one assumes that originally the VPA is homogeneously distributed along the TiO_2 matrix and one would expect that if the crystallization process is faster than the diffusion of VPA in the matrix, the partition of VPA between the amorphous and crystalline zones will correspond to the fraction crystalline versus amorphous phase prevailing. The VPA within a crystalline region should be less mobile than in the amorphous regions and therefore the samples with higher crystallinity must present a slower kinetics of liberation than the more

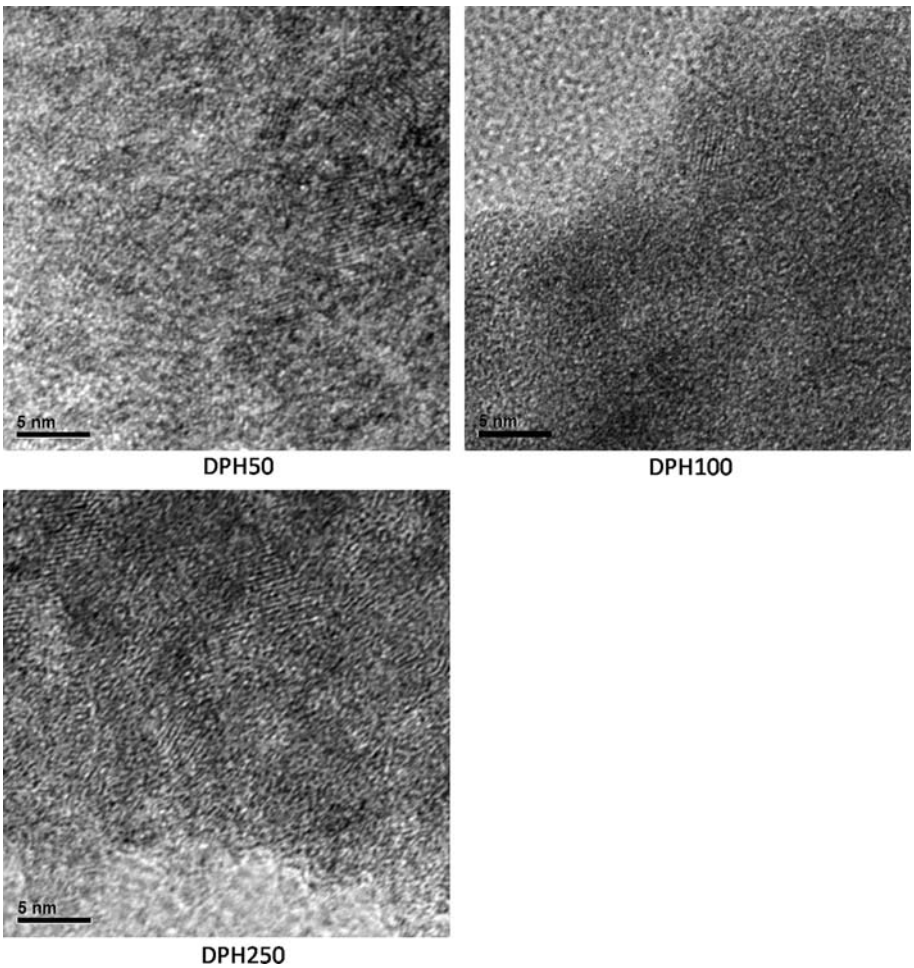

Fig. 4 HRTEM of samples of TiO_2 with different contents of DPH

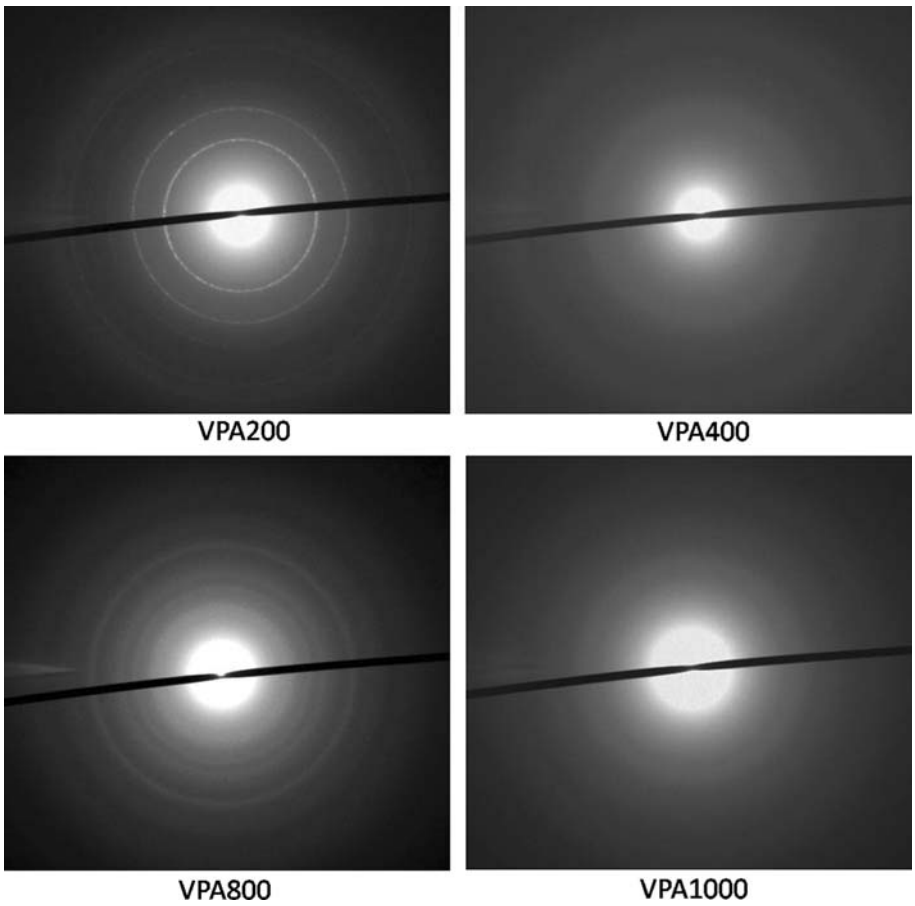

Fig. 5 Electron diffraction patterns of samples of TiO_2 with different contents of VPA

amorphous ones. Some evidence on how attached is VPA to TiO_2 is provided by solid state NMR. Figure 8 shows three NMR spectra of pure VPA, VPA1000 and VPA800. For pure VPA the spectra shows a signal at 15.42 ppm attributed to the methyl groups, followed by a signal at 21.55 and 34.39 ppm corresponding to the methylene groups in VPA. The methine group gives a signal at 47.62 ppm and finally the carbonyl group is displaced at 184.54 ppm. For VPA1000 it is observed the same signal pattern, with the exception of a new signal at 77.9 ppm which has not yet been identified. The spectra are slightly chemically shifted due to the interaction with the TiO_2 matrix. At 186.34 ppm there is a small broader signal of the carbonyl group, indicative of a less mobile group (short relaxation time). One should expect that the stronger interaction of VPA with TiO_2 should be through its carbonyl group, limiting its mobility, which is consistent with the NMR spectra. For VPA800 the 186.34 ppm signal disappears showing an even stronger interaction of the VPA with the titania matrix. This should be expected if the VPA is preferentially within a crystalline phase, consistent with the results found by the electron diffraction patterns where VPA800 is more crystalline than VPA1000. The differences between VPA800 and VPA1000 in pore diameter and surface area are negligible as shown in Table 2 (taken from Ref. [6]). Taking into account that both samples were prepared in the same way, with a 8:1:8 water/alkoxide/alcohol molar ratio, and that the degree of hydroxylation is mainly governed by the molar ratio between water and alkoxide, one can assume that the difference in VPA concentration in these samples will not affect their degree of hydroxylation. Hence the only relevant factors influencing the drug release between these samples are nanocrystallinity and drug concentration gradients. One observes that in the long term delivery regime, VPA1000 has a larger release rate than VPA800, which will be consistent with both a larger concentration of VPA and a greater mobility of the drug in VPA1000 due to its dominant amorphous state. However, in the early delivery (less than 16 h) this is not the case, implying that there must be other mechanisms ruling the rate of liberation at short times such as the amount of VPA adsorbed at the surface of the grains forming the reservoir, the total surface of the macropores of the reservoir (pores formed by the agglomeration of grains), etc.

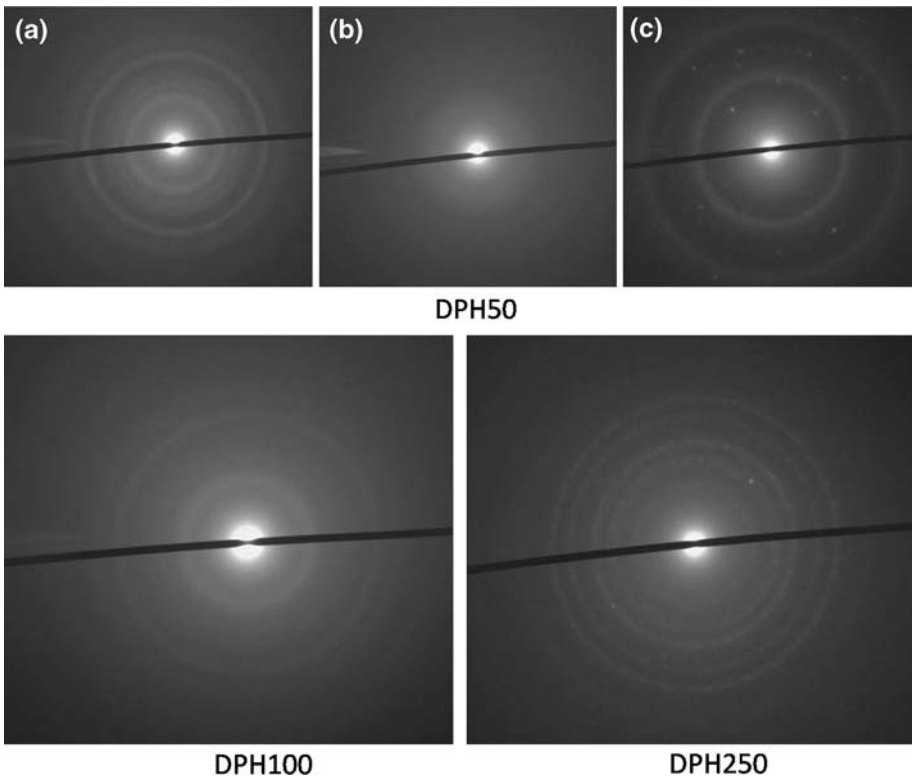

Fig. 6 Electron diffraction patterns of samples of TiO_2 with different contents of DPH. For DPH50, three different regions are shown

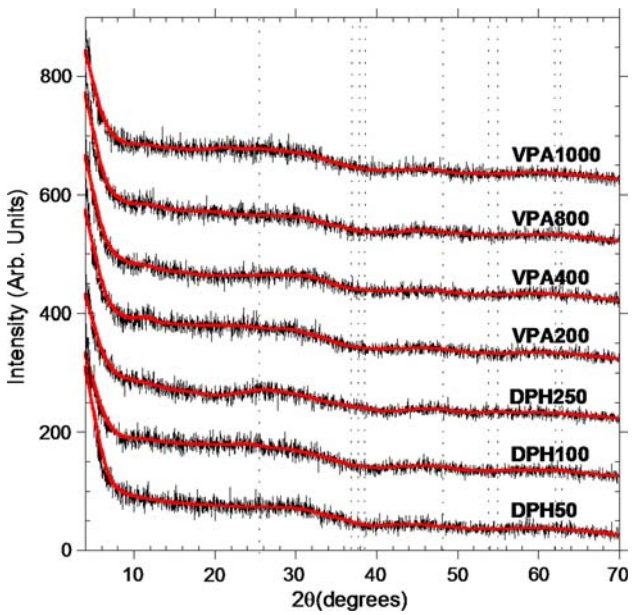

Fig. 7 XRD on samples of TiO_2 with different content of VPA and DPH

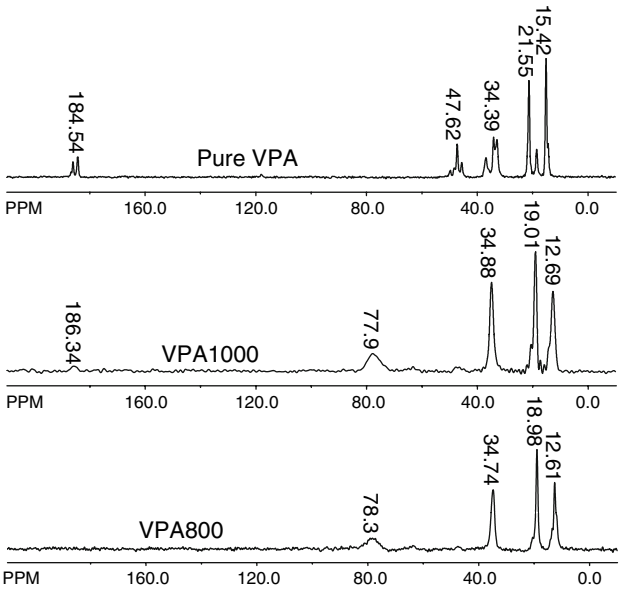

Fig. 8 Solid state NMR on VPA, VPA1000, and VPA800

VPA400 has a larger pore area than both VPA800 and VPA1000 (~24%) and 8.5% larger pore diameter than VPA1000. For long term delivery the rate of drug liberation is substantially lower than VPA1000. Both VPA400 and VPA1000 are predominantly amorphous and therefore in this regime the drug concentration is the dominating factor determining the rate of drug liberation. However, in this long term regime, VPA400 and VPA800 have approximately the same delivering rate implying that the lower concentration of VPA in VPA400 is compensated

Table 2 A comparison of the best fit value for the surface areas *S* and pore diameter for VPA obtained using the Joyner *n* equation

VPA (mg)	*S* (m^2/g) Joyner et al.	Pore diameter (nm) Joyner et al.
0	504	4.0
200	442	3.8
400	593	3.8
800	477	3.6
1000	473	3.5

Adapted from [6] with permission

with a greater effective diffusion rate due to its predominantly amorphous character and larger pore and surface area. At short times possibly other mechanisms associated with grain size, total surface of the grain in the reservoir intervene and complicates a mechanistic interpretation of this regime.

As was mentioned before, the presence of phenytoin does not change the TiO_2 textural parameters. It is also assumed, as before, that the hydroxylation of the sample depends mainly on the molar ratio between TiO_2 and water and therefore one expects the same degree of hydroxylation in all the samples. This again leaves two factors ruling the drug delivery, nanocrystallinity and drug concentration gradients. The amount released follows the same order in short term as in long term drug liberation. This order is defined by the weakly adsorbed DPH liberation within the first 2 h together with the differences in short term kinetics between the samples. In the first 24 h the fastest rate of delivery corresponds to sample DPH100 and the slowest is DPH250. From the diffraction patterns shown in Fig. 6 it is evident that sample DPH250 is more crystalline than DPH100. Therefore DPH will have a greater effective diffusion rate in DPH100 as compared with DPH250. In spite of the concentration differences between the samples, nanocrystallinity in this case has a retarding effect on drug release. DPH50 has the lowest drug concentration yet has a higher drug release rate than DPH250. As shown in Fig. 6, DPH50 is rather heterogeneous; in some regions one finds a sufficient number of nano crystals that scatter giving rise to continuous ring diffraction pattern (DPH50a), in others is highly amorphous (DPH50b) and finally, there are zones where the number of crystals is low producing a discrete spot type diffraction pattern (DPH50c). Qualitatively one might state that DPH50 is sufficiently amorphous to have a larger delivery rate than DPH250.

In vivo studies

For the reference group of rats with a drugless TiO_2 reservoir, all six rats kept on having epileptic events (Crisis–Tonic–Clonic–Generalized CTCG), so no curative effect can be attributed to the empty reservoir. The results with DPH were not satisfactory since their efficiency in preventing further CTCG's was poor. Here are presented only the results with DPH100 for comparison. In the case of VPA, the results were highly promising reaching a 96% efficiency for VPA200. In contrast, the implants with VPA1000 only were effective in 75% of the cases while VPA400 in 83% of the rats implanted. This implies that the amount of VPA included was not the relevant factor but the rate at which this is delivered and probably also the early fast delivery rate. Unfortunately this study did not include an in vitro kinetic study for sample VPA200 nor an in vivo test of VPA800. However, given the interpretation of the kinetic studies, nanocrystallinity played an important role in the rate of delivery of VPA. VPA200 has distinctive well defined diffraction patterns, from which we infer that nanocrystallinity together with the lower drug concentration will play a retarding effect and therefore we should expect a lower rate of delivery than VPA400 and a smaller initial overshoot such as was the case of VPA800. Figure 9 summarizes the results of the study made with the different concentration of VPA.

A comparative histological study (Fig. 10) shows that the nerve cells are not adversely affected by the presence of the reservoir. The interfacial area between the device and the surrounding tissue is devoid of inflammatory areas. This observation suggests that these ceramic implants can safely be used to deliver drugs to the damaged areas of the brain.

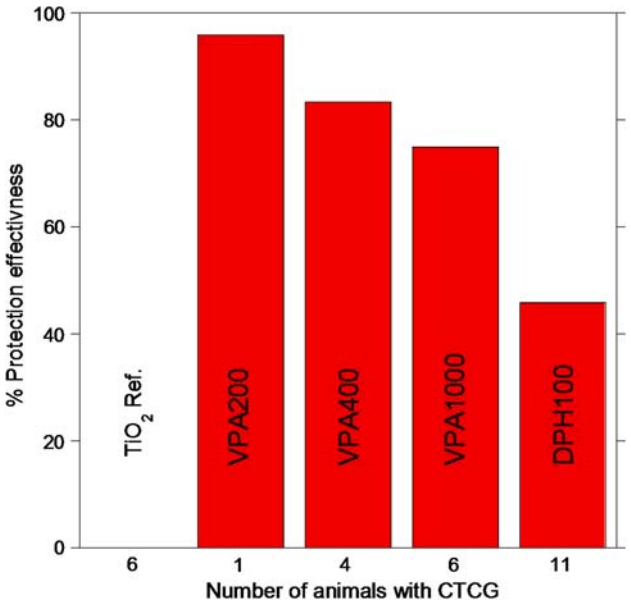

Fig. 9 Percent of protection of the different implants against Crisis–Tonic–Clonic–Generalized (CTCG) on Winstar rats which were previously chemically induced epileptic convulsions following the Kindling model. The number (*n*) of animals per sample tested was 24, except for the reference of TiO_2 where $n = 6$

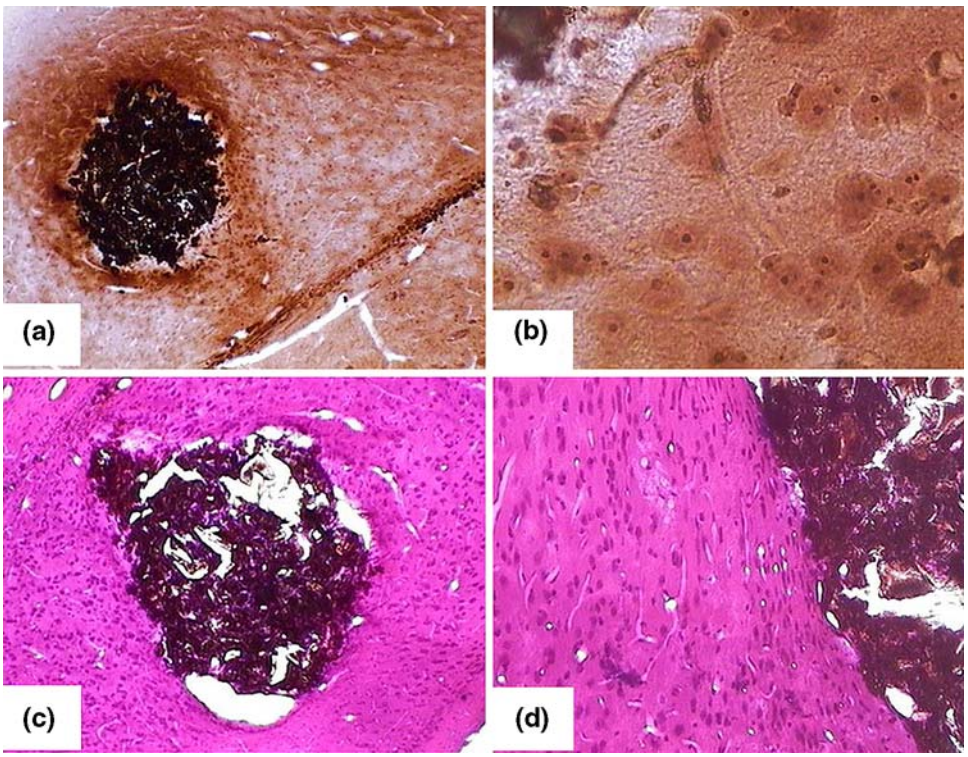

Fig. 10 Comparative histological study. **a** overall view of an histological section with the reservoir (20×); **b** The same as (**a**) at 100×; **c** Glial response to inflammation of the tissue in the neighborhood of the reservoir (20×); **d** Amplified limiting zone in (**c**) at 100×

Conclusions

The short term drug delivery of both VPA and DPH is well described by a first order kinetics with the exception of VPA800 which follows a zero order kinetics (linear law). The general trends of the long term drug liberation could be explained qualitatively in terms of two competing factors, nanocrystallinity versus drug concentration gradients.

In samples with the same textural parameters and hydroxylation such as VPA800 and VPA1000, the only differences between these samples are: their drug content and the degree of nanocrystallization as inferred by the electron diffraction patterns of the samples. It was shown by NMR that VPA was less mobile in VPA800 than in VPA1000, confirming that VPA is more attached to the TiO_2 matrix as crystallinity increases. This fact implied that the presence of nanocrystals had a retarding effect in the drug liberation. The pattern followed by the different kinetic curves in terms of the amount liberated at long times is defined by the weakly adsorbed VPA liberation within the first 2 h together with the differences in short term kinetics between the samples. However, in the short term kinetics of VPA samples other factors intervene in addition to the ones mentioned.

For DPH the amount released follows the same order in short term as in long term drug liberation. This order is defined by the weakly adsorbed DPH liberation within the first 2 h together with the differences in short term kinetics between the samples. Short term and some features of long term kinetics could be understood also in terms of the retarding effect of crystallinity on drug liberation and the concentration gradients associated with the initial loading of the drug.

In vivo studies revealed that a more crystalline sample as VPA200 was more effective in preventing further epileptic events than samples with a higher content of VPA but predominantly amorphous as in the case of VPA400 and VPA1000.

Acknowledgements The authors gratefully acknowledge financial support from CONACYT, The National Institute of Neurosurgery and Neuroscience of Mexico and the Universidad Autónoma Metropolitana (México). The authors will like also express their gratitude to Atilano Gutiérrez C. and Marco Antonio Vera R. for their support in the NMR studies here presented and to Víctor Hugo Lara for the X-Ray runs included in the present work.

References

1. Lopez T, Basaldella EI, Ojeda ML et al (2006) Opt Mater 29:75
2. Benoit J-P, Faisanta N, Venier-Juliennea M-C, Menei P (2000) J Controlled Release 65:285
3. Hoffman A (2008) J Controlled Release 132:153

4. Lopez T, Manjarrez J, Rembao D et al (2006) Mater Lett 60:2903
5. Lopez T, Ortiz E, Quintana P et al (2007) Colloids Surf A 300:3
6. Peterson A, Lopez T, Ortiz E, Gonzalez RD (2007) Appl Surf Sci 253:5776
7. United States Pharmacopoeia Convention, Inc (2007) The United States Pharmacopoeia 30. The National Formulary 25, Arabswell, pp 1445–1448
8. Goddard GV (1967) Nature 214:1020
9. Toga M, Samai M, Payne BA (1989) Brain Res Bull 22:323
10. Morimoto K, Fahnestock M, Racine RJ (2004) Prog Neurobiol 73:1